

Analytical calculation of slip flow in lattice Boltzmann models with kinetic boundary conditions

M. Sbragaglia¹ and S. Succi²

¹ Dipartimento di Fisica and INFN, Università "Tor Vergata",

Via della Ricerca Scientifica 1, I-00133 Roma, Italy

² Istituto per le Applicazioni del Calcolo, CNR,

Viale del Policlinico 137, I-00161, Roma, Italy

February 8, 2008

Abstract

We present a mathematical formulation of kinetic boundary conditions for Lattice Boltzmann schemes in terms of reflection, slip, and accommodation coefficients. It is analytically and numerically shown that, in the presence of a non-zero slip coefficient, the Lattice Boltzmann flow develops a physical slip flow component at the wall. Moreover, it is shown that the slip coefficient can be tuned in such a way

to recover quantitative agreement with analytical and experimental results up to *second* order in the Knudsen number.

1 Introduction

Over the last decade, discrete kinetic methods, and most notably the Lattice Boltzmann (LB), have known a significant growth for the simulation of a variety of complex flows [1]. One of the most valuable properties of the LB method is its flexibility [11], and easy set up of boundary conditions for complex geometries. Such a flexibility stems from the fact that the LB dynamics proceeds along rectilinear trajectories, so that LB shares the computational and conceptual simplicity of particle methods. On the other hand, since the LB dynamics typically involves more dependent variables (discrete distributions) than hydrodynamic fields, the mathematical formulation of boundary conditions is left with some ambiguity, and a systematic treatment of the subject is still lacking. As a result, the issue of boundary conditions has become one of the most active areas of recent LB research. This is especially true for the highly debated question of the applicability of LB methods to microfluidic applications [2]. As recently shown by Ansumali and Karlin, [3], much can be gained in patterning LB boundary conditions after the time-honored procedures developed in continuum kinetic theory [4]. Based on the same philosophy, in this work we present a general class of homogeneous and isotropic boundary conditions for lattice Boltzmann models living on regular

lattices. This class represents a lattice realization of most popular boundary conditions in continuum kinetic theory, that is diffuse boundary conditions with and without accommodation. In this work, special emphasis is placed on the issue of slip flow at the boundary, which plays a central role in microfluidic applications [5]. Analytical expressions for the slip flow are derived for a broad class of boundary conditions and compared with numerical simulations. Excellent agreement between numerical and analytical results is found over a wide range of parameters.

2 Formulation of the boundary condition problem

For the sake of concreteness, we shall refer to the two-dimensional nine-speed D2Q9 model [10], although the proposed analysis can be extended in full generality to any other discrete-speed model living on a regular lattice (for example, the three-dimensional D3Q19 scheme shall be used for comparison with numerical details).

We begin by considering the lattice Boltzmann equation in the following form:

$$f_i(\vec{x} + \vec{c}_i \delta_t, t + \delta_t) - f_i(\vec{x}, t) = -\frac{1}{\tau}(f_i(\vec{x}, t) - f_i^{(eq)}(\rho, \vec{u})) + \frac{\delta_x}{c^2} F g_i \quad (1)$$

where \vec{c}_i ($i = 0, 1, \dots, 8$) is a discrete set of velocities:

$$\vec{c}_\alpha = \begin{cases} \vec{c}_0 & = & (0, 0)c \\ \vec{c}_1, \vec{c}_2, \vec{c}_3, \vec{c}_4 & = & (1, 0)c, (0, 1)c, (-1, 0)c, (0, -1)c \\ \vec{c}_5, \vec{c}_6, \vec{c}_7, \vec{c}_8 & = & (1, 1)c, (-1, 1)c, (-1, -1)c, (1, -1)c. \end{cases}$$

The external source must inject zero mass and ρF units of momentum per unit volume and time. This results in the following constraints on the forcing coefficients g_i :

$$\sum_i g_i \vec{c}_i = 0 \quad \sum_i g_i \vec{c}_i \cdot \vec{c}_i = 1.$$

These constraints can be satisfied by choosing $g_1 = -g_3$ and $g_5 = g_8 = -g_7 = -g_6$, thus leaving us with one free parameter, say g_5 .

We wish to emphasize that since the forcing term is associated with external forces, the $\frac{\vec{F}}{m} \cdot \frac{\partial f}{\partial \vec{v}}$ operator in the Boltzmann equation, there is no reason why g_5 should take the same value in the bulk and at the boundary. As a result, g_5 can be treated as an additional degree of freedom to describe fluid-wall interactions.

The amplitude of the hydrodynamic forcing is chosen in such a way that, if the boundary velocity is zero, it reproduces a Poiseuille flow with centerline speed u_0 :

$$F = \frac{8\nu u_0}{H^2} \tag{2}$$

where $H = N_y \delta_y$ is the channel height. Discrete space and time increments are $\delta_x = \delta_y, \delta_t$, with $c = \frac{\delta_x}{\delta_t}$, and the equilibrium distribution is given by:

$$f_i^{(eq)}(\rho, \vec{u}) = w_i \rho \left[1 + \frac{(\vec{c}_i \cdot \vec{u})}{c_s^2} + \frac{1}{2} \frac{(\vec{c}_i \cdot \vec{u})^2}{c_s^4} - \frac{1}{2} \frac{u^2}{c_s^2} \right] \quad (3)$$

with $w_0 = 4/9$, $w_{1,2,3,4} = 1/9$, $w_{5,6,7,8} = 1/36$ and $c_s^2 = \sum_i w_i c_i^2 = c^2/3$ the lattice sound speed. We consider a system whose y -coordinates lie between $[0, N_y \delta_y]$, N_y being the number of grid points with solid walls located at $-\frac{1}{2}\delta_y$ (south wall), and $N_y \delta_y + \frac{1}{2}\delta_y$ (north wall). In the following, we will refer to the north wall in order to study the boundary condition problem. A general way of formulating the boundary conditions is:

$$f_j(\vec{y}) = \sum_i \mathcal{K}_{j,i}(\vec{x}, \vec{y}, t) f_i(\vec{x}) \quad (4)$$

where the matrix $\mathcal{K}_{j,i}$ is the discrete analogue of the boundary scattering kernel expressing the fluid-wall interactions. In the above $\vec{y} = \vec{x} + \vec{c}_i$ runs over the surface of the wall and the indices i, j stand for incoming and outgoing velocities respectively ($j = 4, 7, 8$ and $i = 2, 5, 6$ for the specific case of D2Q9)). To guarantee conservation of mass and normal momentum, the following sum-rule applies:

$$\sum_j \mathcal{K}_{j,i} = 1 \quad (5)$$

and upon the assumption of stationarity of the fluid-wall interaction, we can drop the dependence on t and write:

$$f_j = \sum_i \mathcal{K}_{j,i} f_i. \quad (6)$$

We now focus our attention on the isotropic homogeneous case. The most general form for $\mathcal{K}_{j,i}$ is:

$$\mathcal{K}_{j,i} = \mathcal{K}_{j,i}(|\hat{c}_i \cdot \hat{c}_j|, |\hat{c}_i \cdot \hat{n}|) \quad (7)$$

where \hat{n} is the outward unit normal to the surface boundary. The dependence on the second argument is necessary to develop a non-zero slip component in the stream-wise direction.

For the case of D2Q9 (same goes for D3Q19), the quantity $|\hat{c}_i \cdot \hat{n}|$ can take only two values, related to the two only possible angles that can be formed between a generic incoming velocity and the normal \hat{n} , in our case $\alpha_1 = \frac{3}{4}\pi$ and $\alpha_2 = \pi$. Explicitly,

$$\begin{pmatrix} f_7(x, N_y \delta_y + \delta_y) \\ f_4(x, N_y \delta_y + \delta_y) \\ f_8(x, N_y \delta_y + \delta_y) \end{pmatrix} = \mathcal{K} \begin{pmatrix} f_5(x - \delta_x, N_y \delta_y) \\ f_2(x, N_y \delta_y) \\ f_6(x + \delta_x, N_y \delta_y) \end{pmatrix} \quad (8)$$

where

$$\mathcal{K} = \begin{pmatrix} \mathcal{K}_{\pi, \alpha_1} & \mathcal{K}_{\frac{3}{4}\pi, \alpha_1} & \mathcal{K}_{\frac{\pi}{2}, \alpha_1} \\ \mathcal{K}_{\frac{\pi}{2}, \alpha_2} & \mathcal{K}_{\pi, \alpha_2} & \mathcal{K}_{\frac{\pi}{2}, \alpha_2} \\ \mathcal{K}_{\frac{\pi}{2}, \alpha_1} & \mathcal{K}_{\frac{3}{4}\pi, \alpha_1} & \mathcal{K}_{\pi, \alpha_1} \end{pmatrix}. \quad (9)$$

Under the assumption of Stokes-flow, it can be shown that in the limit of zero spacings, the above scattering kernel provides an analytical expression for the slip velocity that, in the continuum limit of small time and space increments, reads:

$$u_{slip} = A_{\mathcal{K}} K n \left| \frac{\partial u_x}{\partial \hat{n}} \right|_{wall} + B_{\mathcal{K}} K n^2 \left| \frac{\partial^2 u_x}{\partial \hat{n}^2} \right|_{wall} \quad (10)$$

where

$$A_{\mathcal{K}} = \left(\frac{1 - \mathcal{K}_{\pi, \alpha_1} + \mathcal{K}_{\frac{\pi}{2}, \alpha_1}}{1 + \mathcal{K}_{\pi, \alpha_1} - \mathcal{K}_{\frac{\pi}{2}, \alpha_1}} \right) \frac{c}{c_s}$$

$$B_{\mathcal{K}} = \frac{12g_1}{(1 + \mathcal{K}_{\pi, \alpha_1} - \mathcal{K}_{\frac{\pi}{2}, \alpha_1})} + \left(\frac{1 - \mathcal{K}_{\pi, \alpha_1} + \mathcal{K}_{\frac{\pi}{2}, \alpha_1}}{1 + \mathcal{K}_{\pi, \alpha_1} - \mathcal{K}_{\frac{\pi}{2}, \alpha_1}} \right) \left(12g_5 - \frac{c^2}{c_s^2} \right).$$

In the above, $\tau_f = \frac{\tau}{\delta_t}$ is the relaxation time of the continuum Boltzmann equation (proportional to the Knudsen number) and \hat{n} is the inward normal to the wall. The case of finite spacings can be treated exactly (see Appendix), but for sake of simplicity, here we report only the continuum case.

We wish to emphasize that what we call here 'slip velocity' is the velocity at the nodes nearest to the wall $((x, -\frac{1}{2}\delta_y)$ and $(x, N_y\delta_y + \frac{1}{2}\delta_y))$; to compute the velocity at the wall, an extrapolation of the parabolic profile at $(x, -\frac{1}{2}\delta_y)$ is required.

Our analytical formula provides the slip velocity dependence on the stresses at the wall, on the Knudsen number and on the matrix elements of the scattering kernel, as well as on the forcing weights along the tangential and diagonal directions, g_1 and g_5 respectively. We now proceed to a more direct physical interpretation in terms of reflection and accommodation coefficients.

2.1 Slip-Reflection model (SR)

The first example involves two parameters r, s , representing the probability for a particle to be bounced back and slipped forward, respectively. The boundary kernel takes the form (see [6]):

$$\mathcal{K} = \begin{pmatrix} r & 0 & s \\ 0 & r+s & 0 \\ s & 0 & r \end{pmatrix}. \quad (11)$$

Obviously, the two parameters are not independent and must be chosen such that $r + s = 1$. In this case the slip velocity (10) reads :

$$u_{slip} = AKn \left| \frac{\partial u_x}{\partial \hat{n}} \right|_{wall} + BK n^2 \left| \frac{\partial^2 u_x}{\partial \hat{n}^2} \right|_{wall} \quad (12)$$

where

$$A = \frac{c}{c_s} \frac{1-r}{r} \quad B = \frac{c^2}{c_s^2} (1 - 4g_5). \quad (13)$$

From the first expression, it is clear that the coefficient A is equivalent to Maxwell's first order slip velocity

$$u_{slip} = \frac{2 - \sigma}{\sigma} Kn \left| \frac{\partial u_x}{\partial \hat{n}} \right|_{wall}$$

with $\sigma = 2r$ [7] the well known Maxwell accommodation coefficient. It should be noted that in the limit of pure bounce-back ($r = 1$) the leading term disappears, and one is left with a purely quadratic dependence on the Knudsen number. This quadratic term stems from the tangential populations f_1 and f_3 ; the independence of the coefficient B of r is due to the fact that the tangential populations are evolved according to the same LB dynamics as in the bulk. We also note that in the limit of pure slip $r \rightarrow 0$, the slip flow tends to diverge, as it must be since this limit corresponds to zero friction at the wall. This contrasts with previous results [6], which reported a finite slip length even at vanishingly small values of r . The explanation is that those results were not converged in time.

It is instructive to compare (12) with the corresponding analytical solution for the fully continuum case (also with a continuum velocity phase space), namely [4]

$$u_{slip} = 1.146 Kn \left| \frac{\partial u_x}{\partial \hat{n}} \right|_{wall} + 0.907 Kn^2 \left| \frac{\partial^2 u_x}{\partial \hat{n}^2} \right|_{wall}.$$

First, we notice that there exists a value of r such that the leading term can be reproduced exactly, that is: $r^* \sim 0.603$. The quadratic term can also be

reproduced exactly by choosing $g_5 = 0.175$ and $g_1 = 0.15$. Note that this choice does not affect the bulk behaviour where the Stokes equation is still valid.

Experimental data on slip flow are sometimes interpreted by assuming a Stokes flow in the bulk, coupled to a second order boundary condition of the form (12). In fact, in this way, upon the integration of the Stokes equation with the second order boundary slip it can be shown that the mass flow rate Q_c of the channel is given by:

$$Q_c = SQ_p \tag{14}$$

with Q_p the Poiseuille mass flow rate and S a dimensionless number called slip coefficient depending on the Knudsen number :

$$S = 1 + 6AKn + 12BK n^2.$$

In recent experimental works [8] the slip coefficient has been calculated for Helium and Nitrogen and a good experimental fit has been obtained with a second order slip at the boundaries that gives $A = 1.2 \pm 0.05$, $B = 0.23 \pm 0.1$ for Helium, and $A = 1.3 \pm 0.05$, $B = 0.26 \pm 0.1$ for Nitrogen. It is interesting to note that both sets of coefficients can be exactly reproduced by our model by choosing $r \sim 0.59$, $g_5 \sim 0.22$, $g_1 \sim 0.06$ and $r \sim 0.59$, $g_5 \sim 0.23$, $g_1 \sim 0.04$ for Helium and Nitrogen respectively. More generally, being subject to the constraint $g_5 \leq 1/4$, our model permits to reproduce second order slip

coefficients in the range $0 \leq B \leq 3$.

2.2 Slip-Reflection-Accommodation model (SRA)

The second example is a straightforward generalization of the previous model, which is characterized by a third parameter, a , related to the presence of wall-relaxation (accommodation) phenomena at the fluid-solid interface. By accommodation we imply that the energy of the incoming and outgoing particles is not the same because the outgoing ones are re-injected into the bulk with equilibrium weights. The SRA boundary kernel reads:

$$\mathcal{K} = \begin{pmatrix} r + aW_2 & aW_2 & s + aW_2 \\ aW_1 & r + s + aW_1 & aW_1 \\ s + aW_2 & aW_2 & r + aW_2 \end{pmatrix} \quad (15)$$

with the normalization constraints:

$$r + s + a = 1$$

and $W_2 = 1/6, W_1 = 2/3$. The presence of the weights W_1 and W_2 is due to the fact that they are the discrete analogue of the perfect accommodation kernel, i.e. a uniform Maxwell distribution at wall temperature. The SRA slip velocity has exactly the same form as (13) with the plain replacement

$$r' = r + a/2.$$

As expected, this implies that the accommodation coefficient a results in a smaller slip flow and this shows that the SRA model is basically equivalent to the SR one.

It is known from continuum kinetic theory that a single accommodation coefficient is not sufficient for the quantitative interpretation of experimental data. To cope with this problem, nearly four decades ago Cercignani and Lampis proposed a generalization of Maxwell’s diffuse-boundary model which includes two accommodation coefficients, normal and tangential to the walls [9]. The lattice analogue of the Cercignani-Lampis kernel is readily computed. However, the analysis shows that only the accommodation along the tangential direction plays a role, while the one along the normal direction disappears. This is a pathology of all lattice models where incoming and outgoing normal velocities have the same magnitude. Therefore, we shall not consider this model any further in this work but the use of the lattice Cercignani-Lampis kernel might bear an interest for the case of thermal LB schemes.

3 Numerical validation

We now present a numerical study aimed at validating our analytical results for the *SR* and *SRA* kernels. To this purpose, we have performed numerical simulations of a channel flow with the $3d$ lattice Boltzmann model with 19 discrete speeds (D3Q19). First, we consider the case of equi-balanced exter-

nal forcing among all biased populations (the equivalent of $g_5 = g_1$ in the case of $D2Q9$). The channel has dimensions $N_x = 64, N_y = 32, N_z = 32$, the Knudsen number is $Kn = 0.08$ and the forcing has been fixed so as to reproduce a center-channel velocity $u_0 = 0.03$ in the limit of a Poiseuille flow (2).

In Figure 1 we show the center-channel profile in the stream-wise direction for the RS case. By varying the free parameter r between 0.1 and 1 the profile “shifts” with no changes in its concavity, which is fixed by the external forcing term F and the viscosity ν , both kept constant in the simulations.

In Figure 2 we present a comparison between the slip velocity, as extracted from numerical data, and our analytical results for the *discrete* case (see Eq. (29) in the Appendix). An excellent agreement between numerical and analytical results in the range $0.1 < r < 1$ is clearly observed. For sake of completeness we have also compared the mass flow rate normalized to the pure bounce back case with our analytical solution (inset of Figure 2) and, as expected, also here an excellent agreement is found.

In Figure 3, we show the effect of the accommodation parameter a in reducing the slip flow. The parameter is chosen as $a = 0.3$ and the values of r, s are chosen accordingly. The slip velocity is the same as the case SR , only with a renormalized reflection coefficient $r' = r + a/2$ as can be clearly seen in the inset.

We have also performed a set of numerical simulations with different repartitions of the external forcing term, in order to study the slip properties

as a function of the Knudsen number. In the case of SR kernels, fixing the bounce-back parameter to $r = 0.59$ and the center-channel velocity to $u_0 = 0.01$ in the limit of Poiseuille flow, we have studied the slip velocity as a function of the Knudsen number Kn in the range $0 < Kn < 0.8$. We have chosen an unbalanced bipartition with a forcing coefficient equal to 0.23 for the incoming populations in order to reproduce (see Figure 4) the experimental results showed in [8] for the case of Helium; the numerical results confirm our analysis and are indistinguishable from experimental data up to second order terms in the Knudsen number.

4 Conclusions

Summarizing, we have presented a unified formulation for a broad class of homogeneous and isotropic boundary conditions for lattice Boltzmann models living on regular lattices. Analytical expressions for the slip flow at the fluid-solid boundary have been derived and successfully compared with numerical simulations of three-dimensional channel flow. The main conclusion is as follows: by allowing a non-zero slip coefficient, the Lattice Boltzmann flow develops a slip flow component which can be matched exactly to analytical and experimental data up to second order in the Knudsen term, well inside the transition regime ($0 < Kn < 0.8$). This means that the lattice Boltzmann scheme with kinetic boundary conditions *can* be used to predict slip flow at finite Knudsen numbers well beyond the strict hydrodynamic limit.

Of course, the extension of the present model to more realistic situations, involving complex geometries and/or inhomogeneities [12, 13] and thermal effects [14] remains an open issue.

Acknowledgments

We are grateful to S. Ansumali, R.Benzi, I. Karlin and F.Toschi for useful discussions. We thank L. Biferale for a careful and critical reading of the manuscript.

5 Appendix

We impose stationary condition on the node $(x, N_y\delta_y)$ and, under the assumption of homogeneity, we drop the x dependence and write :

$$\begin{cases} \mathcal{K}_{\pi,\alpha_1}f_5(N_y\delta_y) + \mathcal{K}_{\frac{3}{4}\pi,\alpha_1}f_2(N_y\delta_y) + \mathcal{K}_{\frac{\pi}{2},\alpha_1}f_6(N_y\delta_y) - \frac{\delta_x}{c^2}Fg_5 = f_7(N_y\delta_y) \\ \mathcal{K}_{\frac{\pi}{2},\alpha_1}f_5(N_y\delta_y) + \mathcal{K}_{\frac{3}{4}\pi,\alpha_1}f_2(N_y\delta_y) + \mathcal{K}_{\pi,\alpha_1}f_6(N_y\delta_y) + \frac{\delta_x}{c^2}Fg_5 = f_8(N_y\delta_y) \\ (f_1 - f_3)(N_y\delta_y) - (f_1^{(eq)}(\rho, \vec{u}) - f_3^{(eq)}(\rho, \vec{u})) = 2F\tau\frac{\delta_x}{c^2}g_1. \end{cases} \quad (16)$$

We can now write for the velocity in the x -direction at the height $(N_y\delta_y)$:

$$\frac{1}{3}\rho u_{slip} = (2g_1\tau + 2g_5)F\frac{\delta_x}{c} + c(1 - \mathcal{K}_{\pi,\alpha_1} + \mathcal{K}_{\frac{\pi}{2},\alpha_1})\zeta(N_y\delta_y) \quad (17)$$

with

$$f_5(x, y) - f_6(x, y) = \zeta(y). \quad (18)$$

Using the equations for f_5 and f_6 in the bulk, and under the stationarity assumption, we obtain:

$$\begin{cases} f_5(x + c\delta_t, y + c\delta_t) - f_5(x, y) = -\frac{1}{\tau}(f_5(x, y) - f_5^{(eq)}(\rho, \vec{u})) + \frac{\delta_x}{c^2}Fg_5 \\ f_6(x - c\delta_t, y + c\delta_t) - f_6(x, y) = -\frac{1}{\tau}(f_6(x, y) - f_6^{(eq)}(\rho, \vec{u})) - \frac{\delta_x}{c^2}Fg_5. \end{cases} \quad (19)$$

Dropping the x dependence (homogeneity), upon the definition (18), we have

$$\zeta(y) - \zeta(y - c\delta_t) = -\frac{1}{\tau}\zeta(y - c\delta_t) + \frac{\rho u_x(y - c\delta_t)}{6\tau c} + 2Fg_5 \frac{\delta_x}{c^2} \quad (20)$$

In the limit $\delta_x, \delta_y, \delta_t \rightarrow 0$ we obtain an *O.D.E.* which can be solved exactly .

However, by considering finite spacings such that $\delta_x = \delta_y = c = 1$, we have:

$$\zeta(j) - \zeta(j - 1) = -\frac{1}{\tau}\zeta(j - 1) + \frac{\rho u_x(j - 1)}{6\tau} + 2Fg_5 \quad 1 \leq j \leq N_y \quad (21)$$

where j stands runs over the channel height. This finite difference equation can be solved exactly. The solution can be divided in two terms: the homogeneous term $\zeta^{hom}(j)$ and a particular term $\zeta^{part}(j)$. For the homogeneous term we have:

$$\zeta^{hom}(j) = \left(1 - \frac{1}{\tau}\right)^j \quad (22)$$

while for the particular term we use the method of variation of constants:

$$\zeta^{part}(j) = \left(1 - \frac{1}{\tau}\right)^{j-1} \sum_{k=0}^{j-1} \left(1 - \frac{1}{\tau}\right)^{-k} \left[\frac{\rho u_x(k)}{6\tau} + 2Fg_5\right]. \quad (23)$$

Summing the two contributions (23) and (22) we have an explicit form for the general solution of (21)

$$\zeta(j) = C \left(1 - \frac{1}{\tau}\right)^j + \left(1 - \frac{1}{\tau}\right)^{j-1} \sum_{k=0}^{j-1} \left(1 - \frac{1}{\tau}\right)^{-k} \left[\frac{\rho u_x(k)}{6\tau} + 2Fg_5\right] \quad (24)$$

where C is a constant to be fixed based upon boundary conditions. Since $\zeta(N_y)$ enters in (17), we have:

$$\zeta(N_y) = C \left(1 - \frac{1}{\tau}\right)^{N_y} + \left(1 - \frac{1}{\tau}\right)^{N_y-1} \sum_{k=0}^{N_y-1} \left(1 - \frac{1}{\tau}\right)^{-k} \left[\frac{\rho u_x(k)}{6\tau} + 2Fg_5\right] \quad (25)$$

and under the assumption of low-Knudsen numbers ($N_y/\tau \gg 1$), $\zeta(N_y)$ is well approximated by $\zeta^{part}(N_y)$, since $(1 - \frac{1}{\tau})^{N_y} \rightarrow 0$. As a result:

$$\zeta(N_y) = \left(1 - \frac{1}{\tau}\right)^{N_y-1} \sum_{k=0}^{N_y-1} \left(1 - \frac{1}{\tau}\right)^{-k} \left[\frac{\rho u_x(k)}{6\tau} + 2Fg_5\right] \quad (26)$$

which substituted in (17), and setting $\rho = 1$, returns the following expression for the velocity at the height (N_y):

$$u_{slip} = (6\tau g_1 + 6g_5)F + \frac{1}{2}(1 - \mathcal{K}_{\pi, \alpha_1} + \mathcal{K}_{\frac{\pi}{2}, \alpha_1}) \left[\left(1 - \frac{1}{\tau}\right)^{N_y-1} \sum_{k=0}^{N_y-1} \left(1 - \frac{1}{\tau}\right)^{-k} \left(\frac{u_x(k)}{\tau} + 12Fg_5\right) \right]. \quad (27)$$

Next we impose a low-Reynolds regime, by specifying the velocity field as a (symmetric) parabolic profile:

$$\begin{cases} u_x(j) = aj^2 + bj + u_{slip} & 0 \leq j \leq N_y \\ b = -aN_y & \text{since } u_x(N_y) = u_x(0) \\ a = -\frac{F}{2\nu} & \text{since } \nu\partial_{jj}u_x(j) = -F \end{cases} \quad (28)$$

and we obtain for the slip velocity:

$$u_{slip} = \frac{(12\tau g_1 + 12g_5)F}{(\mathcal{K}_{\pi,\alpha_1} - \mathcal{K}_{\frac{\pi}{2},\alpha_1} + 1)} + \left(\frac{1 - \mathcal{K}_{\pi,\alpha_1} + \mathcal{K}_{\frac{\pi}{2},\alpha_1}}{\mathcal{K}_{\pi,\alpha_1} - \mathcal{K}_{\frac{\pi}{2},\alpha_1} + 1} \right) [12F\tau g_5 + I_1 + I_2] \quad (29)$$

where:

$$I_1 = \frac{a}{\tau} \left(1 - \frac{1}{\tau}\right)^{N_y-1} \sum_{k=0}^{N_y-1} k^2 \left(1 - \frac{1}{\tau}\right)^{-k} \quad (30)$$

$$I_2 = \frac{b}{\tau} \left(1 - \frac{1}{\tau}\right)^{N_y-1} \sum_{k=0}^{N_y-1} k \left(1 - \frac{1}{\tau}\right)^{-k}. \quad (31)$$

References

- [1] R. Benzi, S. Succi, M. Vergassola, Phys. Rep. 222, 145, 1992, D Wolfe-Gladrow, Lattice Gas Cellular Automata and Lattice Boltzmann Model, Springer Verlag, 2000, S. Succi, The Lattice Boltzmann equation, Oxford Univ. Press, Oxford, (2001).
- [2] Y.H. Qian, Y. Zhou, Phys Rev E, 61, 2103, 2000;
X. Nie, G. Doolen, S. Chen, J. Stat. Phys., 107, 29, 2002;

- X. He, Q. Zou, L.S. Luo, M. Dembo, J. Stat. Phys., 87, 115, 1997;
- B. Li and D. Kwok, Phys. Rev. Lett., 90, 124502, 2003;
- C. Lim, C. Shu, X. Niu, Y. Chew, Phys. Fluids, 14, 2299;
- J. Zhou, L. Zhu, L. Petzold, T. Yang, 18th International Parallel and Distributed Processing Symposium (IPDPS 2004), Proceedings, 26-30 April 2004, Santa Fe, New Mexico, USA. IEEE Computer Society 2004, ISBN 0-7695-2132-0, to appear.
- [3] S. Ansumali, I. Karlin, Phys. Rev. E, 66, 026311, 2002.
- [4] C. Cercignani, “Theory and application of the Boltzmann equation”, Scottish Academic Press, 1975.
- [5] C.M. Ho, Y.C. Tai, Annu. Rev. Fluid Mech., 30, 579, 1998; G. Karniadakis, *Microflows*, Springer Verlag, 2001; P. Tabeling, *Introduction a la microfluidique*, 2003.
- [6] S. Succi, Phys. Rev. Lett., 87, 96105, 2002.
- [7] J.C. Maxwell, Phil. Trans. Soc. London, 170, 231, 1867.
- [8] J. Maurer, P. Tabeling, P. Joseph, H. Willaime, Phys. Fluids, 15, 2613, 2003.
- [9] C. Cercignani, M. Lampis, Transp. Theory and Statis. Phys., 1, 101, 1971; F. Sharipov, Europ. J. of Mech. B/Fluids, 22, 145, 2003.

- [10] Y. Qian, D. d'Humières, P. Lallemand, Europhys. Lett. 17, 479, 1992.
- [11] F.J. Higuera, S. Succi, R. Benzi, Europhys. Lett, 9, 345, 1989.
- [12] N.Priezjev, A. Darhuber, S.M. Troian, cond-mat/0405268;
- [13] A. Dupuis, J.M. Yeomans, Future Generation Computer Systems, 20, 993, 2004.
- [14] Y. Zheng, A. Garcia, B. Alder, J. Stat. Phys., 109, 291, 2002.

FIGURE 1

Velocity profiles with SR kernels. We plot the center-channel profile in the stream-wise direction as a function of the normalized distance from the wall $y_{norm} = y/H$, being H the channel height. Different values of the parameters (r, s) are considered. From top to bottom we plot the following cases: $(0.4, 0.6)$, $(0.5, 0.5)$, $(0.7, 0.3)$, $(0.9, 0.1)$. In all simulations the Knudsen number is $Kn = 0.08$ and the forcing term has been fixed to reproduce a center channel velocity $u_0 = 0.03$ in the limit of a Poiseuille flow (2).

FIGURE 2

Slip velocity for the SR kernels. We plot u_{slip} vs r for different values of the bounce back parameter r . The data of numerical simulations (boxes) are compared with the analytical estimate (29) (dotted line). The agreement is excellent all over the range $0.1 < r < 1$. Inset: numerical data ((boxes) representing the mass flow rate normalized to its pure bounce-back value (Q_{norm}) are compared with our analytical estimate (dotted line).

FIGURE 3

Velocity profiles with the SRA kernels. We plot the center channel profile in the stream-wise direction as a function of the normalized distance from the wall $y_{norm} = y/H$, being H the channel height. Different values of the parameters (a, r, s) are considered. We analyze the following plots: $(0.0, 0.5, 0.5)$ (top plot) and $(0.3, 0.5, 0.2)$ (bottom plot). Inset: analysis for the slip velocity in the channel in the case (a, r, s) with $a = 0.3$. The data of numerical simulations (boxes) are compared with the analytical estimate (29) (dotted

line) with a normalized reflection coefficient $r' = r + a/2$. The agreement is excellent all over the range $0.2 < r < 0.7$.

FIGURE 4

Analysis for the slip coefficient (14) in the channel as a function of the Knudsen number. The data of numerical simulations (circles) with a properly unbalanced repartition of the external forcing are compared with the experimental results (triangles) given in [8] and with the analytical expression (14) with $A = 1.2$ and $B = 0.23$ (dotted line). The linear full accommodation case ($u_{slip} = Kn \left| \frac{\partial u_x}{\partial n} \right|_{wall}$) is also plotted for a comparison. Inset: the slip velocity as a function of the Knudsen number is studied with the same repartition of the external forcing as before. We compare the numerical data (circles) with our analytical expression (dotted line) including, as before, terms up to the second order in the Knudsen number. In all the simulations we have used a SR kernel with a bounce back parameter $r = 0.59$.

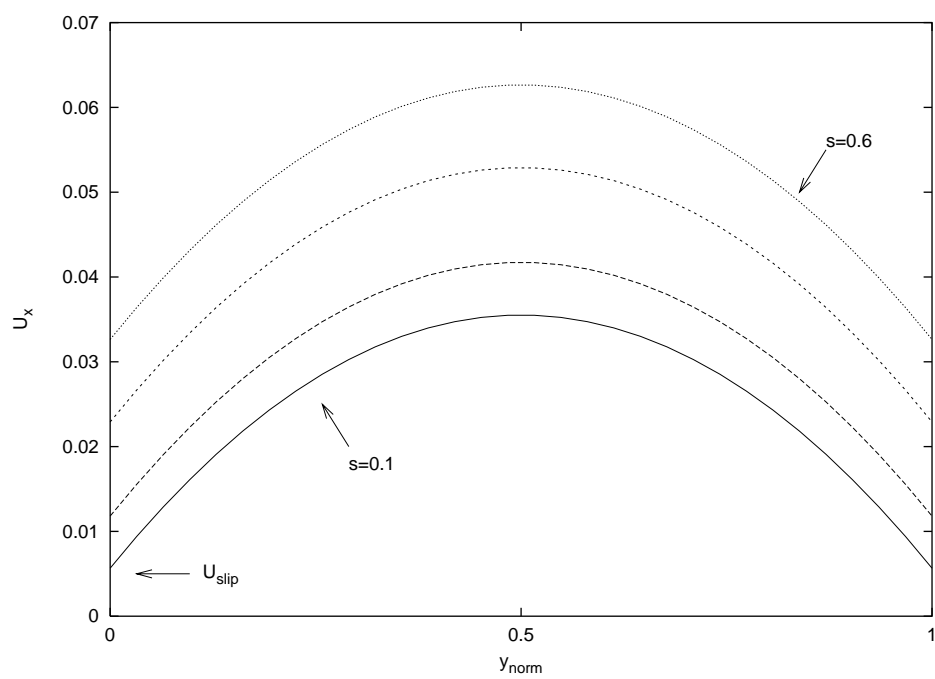


Figure 1:

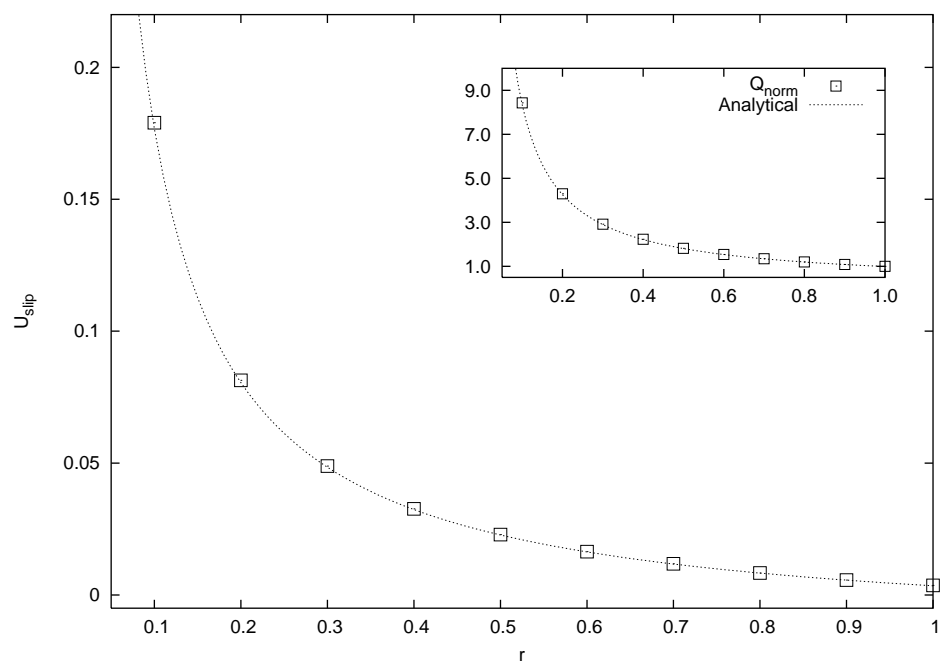


Figure 2:

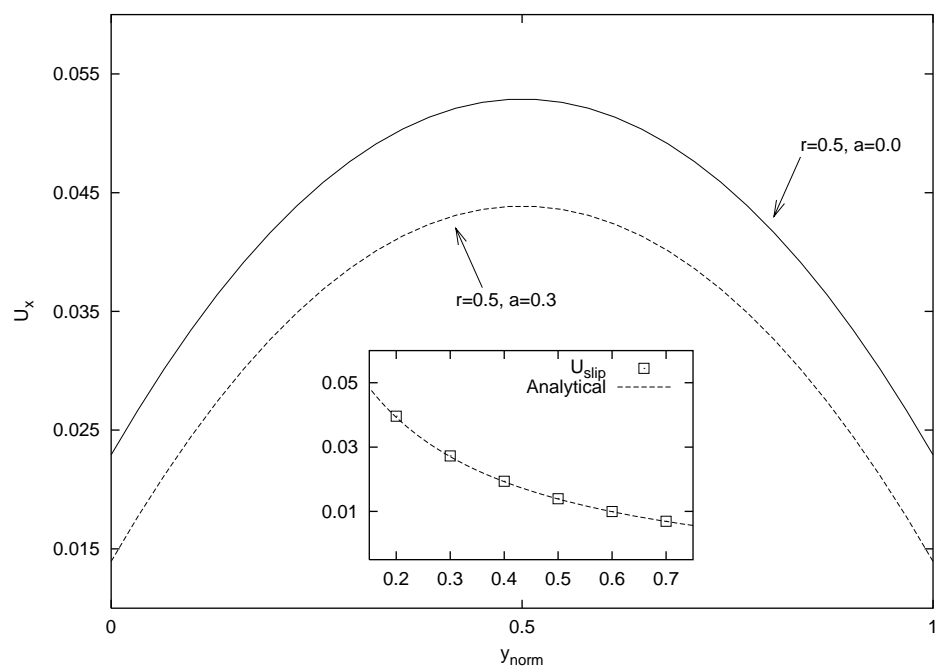


Figure 3:

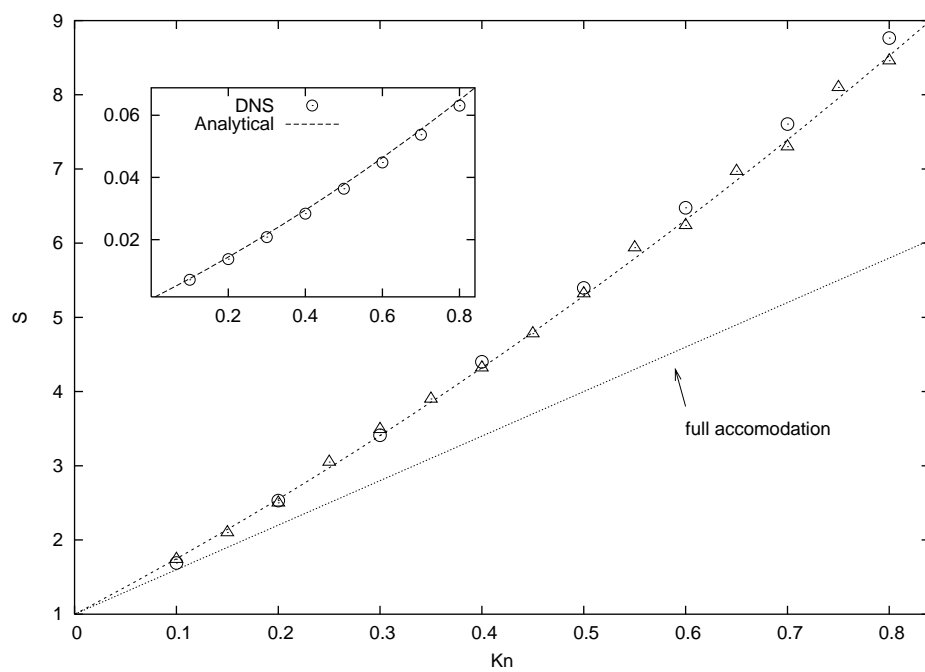


Figure 4: